PASJ: Publ. Astron. Soc. Japan **46**, L131–L136 (1994)

ASCA Detection of Iron Line Emission from the Distant Galaxy Cluster Abell 370

Marshall W. BAUTZ,[1] Richard MUSHOTZKY,[2] Andrew C. FABIAN,[3] Koujun YAMASHITA,[4]
Keith C. GENDREAU,[1] Keith A. ARNAUD,[2] Geoffrey B. CREW,[1] and Yuzuru TAWARA[4]

[1]*Center for Space Research, Massachusetts Institute of Technology, Cambridge, MA 02139, U.S.A.*
Email (MWB): mwb@space.mit.edu
[2]*NASA/Goddard Space Flight Center, Greenbelt, MD 20771, U.S.A.*
[3]*Institute of Astronomy, University of Cambridge, Maddingley Road, Cambridge, CB3 0HA, U.K.*
[4]*Department of Physics, School of Science, Nagoya University, Furo-cho, Chikusa-ku, Nagoya 464-01*

(Received 1994 February 25; accepted 1994 April 12)

Abstract

ASCA observations of the gravitational lens and Butcher-Oemler cluster Abell 370 ($z = 0.37$) give $kT = 8.8 \pm 0.8$ keV and $A = 0.5 \pm 0.1$ cosmic. If the gas were isothermal the implied cluster mass would be $M_{\rm vir} = (1.5 \pm 0.4) \times 10^{15} M_{\odot}$, a value consistent with the optically-determined virial mass. We detect iron K line emission with high confidence. This measurement increases, by a large factor, the lookback time at which the presence of iron in the intracluster medium has been established. The iron abundance is marginally higher than that of low-redshift clusters of similar temperature, so our results are consistent with models in which all enrichment occurs before the epoch corresponding to $z = 0.37$.

Key words: Galaxies: clustering — Galaxies: evolution — Intergalactic medium — X-rays: galaxies

1. Introduction

A number of studies of the cluster X-ray luminosity function suggest that there has been substantial negative evolution in X-ray luminosity since $z \sim 0.1$–0.2 (Edge et al. 1990) and $z > 0.3$ (Gioia et al. 1990; Henry et al. 1992); that is, the bright end of the cluster luminosity function at earlier epochs was underpopulated, relative to the present cluster X-ray luminosity function. However, relatively little is known about the X-ray spectral evolution of clusters. Early inferences from Einstein IPC hardness ratios suggested that the intracluster medium (ICM) is cooler in distant objects (Perrenod, Henry 1981), but more recent analysis of the Einstein data (Wang, Stocke 1993) has not supported this conclusion. Even less is known about the chemical composition of the ICM in distant clusters. Ginga detected iron line emission from clusters as distant as A483 ($z = 0.28$), and within the (relatively large) uncertainties, found the iron abundance to be similiar to that of nearby objects (Arnaud et al. 1991).

ASCA observations of distant clusters promise significant increases in our understanding of clusters of galaxies. Even for objects too distant for detailed spatially resolved X-ray spectroscopy, temperature measurements can constrain the total quantity and spatial distribution of cluster mass (e.g., Cowie et al. 1987; Hughes 1989; Loewenstein 1994). In addition, ASCA can detect line emission with high confidence in distant clusters, and thereby constrain the enrichment history of the intracluster gas.

Abell 370, at $z = 0.37$, is one the most distant and best-studied high-z clusters in the Abell catalog (Abell et al. 1989). The cluster is a luminous X-ray source, with $L_{\rm X} = (1.28 \pm 0.12) \times 10^{45}$ erg s^{-1}, 0.2–4.5 keV (Fabricant et al. 1991). Mellier et al. (1988) report a velocity dispersion of 1350 km s^{-1}, and note that the cluster is similar in many ways to the Coma cluster: it is rich, the galaxy distribution is relatively concentrated, and the optical emission is dominated by two giant ellipticals. A370 exhibits the Butcher-Oemler effect, with a blue galaxy fraction in the range $0.13 \leq f_b \leq 0.21$ (Butcher, Oemler 1984); as many as 50% of the galaxies in the core have optical spectra indicative of recent star formation (Mellier et al. 1988). The cluster is also a spectacular gravitational lens, producing a giant luminous arc (Lynds, Petrosian 1986; Paczynski 1987; Soucail et al. 1987) and possibly other gravitational images as well (Kneib et al. 1993).

2. The X-Ray Data

A370 was observed by ASCA on 1993 July 18. The total useful exposure was about 37500 s. Data from both the SIS and GIS were reduced using standard techniques.

Table 1. Spectral Model Parameters.*

Data set	Raymond-Smith model		Iron line model		
	kT (keV)	Abundance†	kT (keV)	Line centroid‡ Rest frame (keV)	EW# (eV)
SIS	9.4 (8.2–11.1)	0.43 (0.20–0.69)	9.7 (8.2–11.6)	6.64 (6.57– 6.71)	266 (127–468)
GIS	7.8 (6.7–9.2)	0.64 (0.36–0.95)	8.4 (7.3–10.0)	6.57 (6.41–6.76)	426 (252–663)
SIS+GIS	8.8 (7.9–9.7)	0.49 (0.31–0.69)	9.1 (8.1–10.2)	6.65 (6.57–6.71) SIS	323 (154–568) SIS
				6.50 (6.35–6.76) GIS	426 (252–663) GIS

* Cluster restframe values; 90% confidence limits in parentheses.
† Relative to Fe : H = 3.2×10^{-5} by number (Ross, Aller 1976).
‡ Energy of Fe XXV feature for SIS.
# Sum of equivalent widths for Fe XXV and Fe XXVI features for SIS.

Although the observation was conducted with the SIS in 4-CCD mode, most of the cluster emission was imaged by a single CCD in each SIS. Because these particular CCDs (chip 0 in sensor 0 and chip 3 in sensor 1) are the best calibrated at this time, we restrict our analysis to data from these chips. We have integrated the cluster emission in apertures of diameter 5′ and 12.′5 for the SIS and GIS data, respectively. Net counting rates (above background) in these apertures are 4.6×10^{-2} ct s^{-1} and 5.5×10^{-2} ct s^{-1} in the 0.8–8 keV band for the SIS and GIS, respectively.

Accurate background determination is essential for correct spectral analysis of this low-surface brightness source. The instrumental (non-X-ray) backgrounds were determined from multiple exposures to the dark earth. The cosmic X-ray background was determined from exposures to several fields at high galactic lattitude. These fields provide a good estimate of the hard ($E >\sim 0.8$ keV), isotropic component of the background (Gendreau et al. 1994, private communication); the softer backround, however, is known to be anisotropic. For this reason we restrict analysis to energies $E > 0.8$ keV. The measured total (cosmic plus instrumental) background rates in the 0.8–8 keV band are 5.5×10^{-3} ct s^{-1} within a 5′ diameter aperture for the SIS and 1.2×10^{-2} ct s^{-1} within a 12.′5 diameter aperture for the GIS.

Spectral models described below have been fit to each of three data sets: the SIS data alone, the GIS data alone, and data from both sensors. The XSPEC spectral fitting program has been used for all fits. The likelihood statistic (rather than χ^2) has been used as the goodness of fit parameter, since the mean number of counts per pulse-height channel is small. In all cases the source and background are included in the model fit to the data, though the background model parameters have been held fixed at values determined as described above.

The data, best-fit optically thin thermal plasma (Raymond-Smith) model, and background model are shown in figure 1. Fe K line emission is detected with high significance. The temperature and heavy element abundance and their (single parameter 90% confidence) error limits are listed in table 1 and shown in figure 2. In the joint fit to all the data, the SIS and GIS normalizations have been varied independently. Note that, to maximize statistical precision, the results shown in table 1 are taken from two different aperture diameters (5′ for the SIS and 12.′5 for the GIS). Fits to GIS data in 5′ and 12.′5 diameter apertures yield identical model parameters, within the (67% confidence) errors. Note also that the data in this energy range do not tightly constrain the absorbing column, requiring only $N_{\rm H} \leq 3 \times 10^{20}$ cm^{-2} (90% confidence), which is consistent with the 21 cm line measurement of $N_{\rm H} = 2.5 \times 10^{20}$ cm^{-2} (Stark et al. 1992). Accordingly, the fits listed in table 1 have been obtained with the absorbing column density fixed at zero.

To characterize the line emission further, a model consisting of a thermal bremstrahlung continuum and two gaussian-profile emission lines, which model the Kα complexes of Helium-like and Hydrogen-like iron, has been fit to the data (see table 1). The line centroid energies have been fixed in the ratio of 1.045 : 1 when performing the fit. The lower energy resolution GIS data have been fit with a single line component. In the fits of this model to the joint SIS+GIS data set, the line parameters have been allowed to vary separately for the two sensors. At the 90% confidence level, the data are consistent with zero width for each line component, and rest frame energies consistent with H-like and He-like Fe lines (results in table 1 have the line widths constrained to be zero). The equivalent width of each of the line components has been computed separately. The ratio of H-like and He-like line fluxes in the SIS data is consistent with the predictions of the best fit Raymond-Smith model.

Although the SIS and GIS results are consistent at the

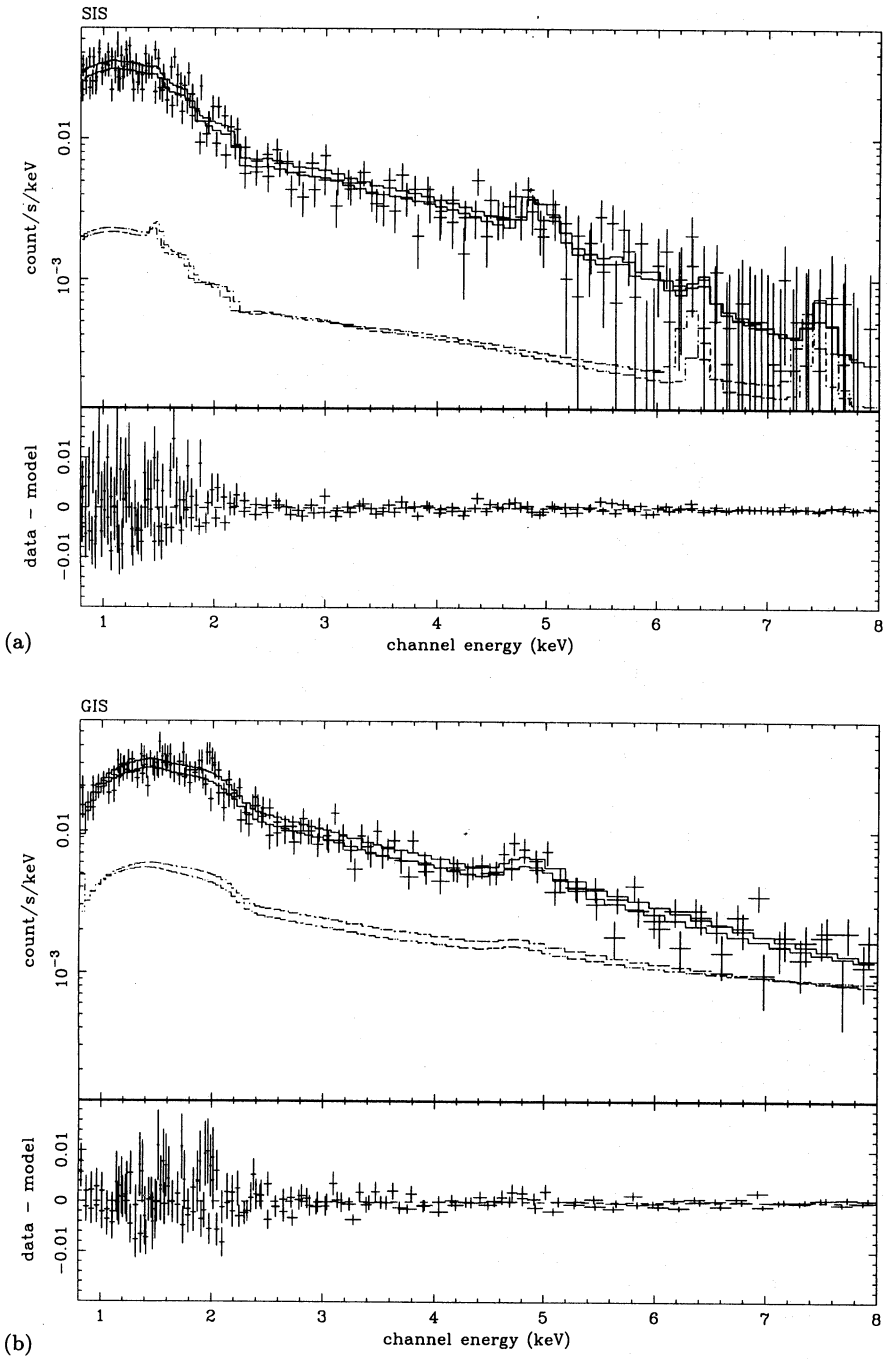

Fig. 1. Observed pulse-height spectra (crosses), best fit ionized thermal plasma (Raymond-Smith) models (solid curves), background models (dashed lines) and residuals (data minus model, lower panel) for a) the SIS (5′ diameter aperture) and b) the GIS (12′.5) diameter aperture. The solid curves indicate the sum of the source and background models. The best-fit source model parameters are listed in table 1. Redshifted iron-K line emission is detected with high confidence. The solid curves include the assumed background model.

90% confidence level, table 1 indicates that the best-fit SIS temperatures are higher than those obtained from the GIS data. When measurements in equal apertures are compared, the difference in measured temperatures is reduced to 0.5 keV, which is within 67% confidence-level errors. The differences in SIS and GIS results listed in table 1 need not reflect a temperature gradient in the source, however. Instead, aperture-size-dependent systematic errors arising from errors in the assumed background flux may be important. In particular, systematic

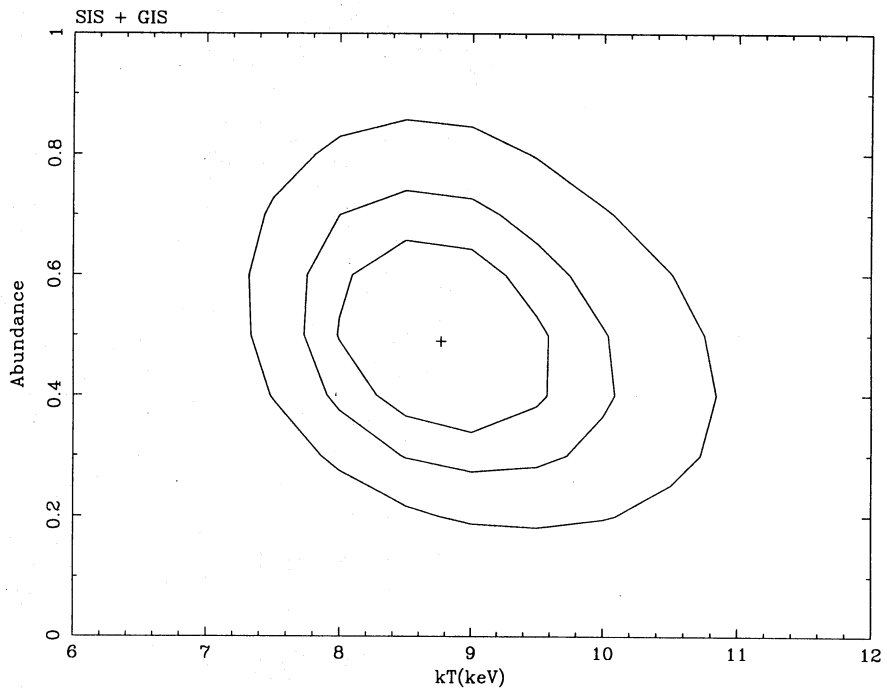

Fig. 2. Contours of constant likelihood (associated with 67%, 90%, and 99% confidence levels) in the abundance-temperature plane for the best-fit Raymond-Smith model fit to data from both the SIS and GIS.

variation of the normalization of the assumed background model over 90% confidence intervals alters the best fit temperatures by approximately ±0.5 keV for the SIS and ±1 keV for the GIS (the GIS results are more sensitive to background errors because the GIS data are taken from a larger aperture.) We estimate that the systematic errors on the temperatures derived from the joint fits to be less than ±1 keV. The abundance measurements are not affected appreciably by these systematic errors.

3. Discussion

We measure the X-ray luminosity of A370 to be $L_X = (1.0 \pm 0.1) \times 10^{45}$ erg s^{-1} in the 2–10 keV band (cluster rest frame) within an aperture 5′ (1.9 Mpc) in diameter (we assume $H_0 = 50$ km s^{-1} Mpc^{-1} and $q_0 = 1/2$ throughout). The corresponding luminosity in the 12.′5 (4.5 Mpc) diameter aperture is $(1.3 \pm 0.1) \times 10^{45}$ erg s^{-1}. The estimated uncertainty in the luminosity is based on the internal consistency of the flux measurements from the two SIS sensors. The Einstein IPC measurement (Fabricant et al. 1991) is $L_X = (1.28 \pm 0.12) \times 10^{45}$ erg s^{-1}, 0.2–4.5 keV, in a 3.5 Mpc diameter aperture. The best-fit ASCA spectrum implies a luminosity in the 0.2–4.5 keV band essentially identical to that in the 2–10 keV band. If we assume that the X-ray surface brightness distribution follows a hydrostatic isothermal model profile with core radius of 0.25 Mpc and $\beta = 0.65$, consistent with the mean values of these parameters in low-redshift clusters (Jones, Forman 1984) we expect $L_X(r < .95 \text{ Mpc})/L_X(r < 1.75 \text{ Mpc}) = 0.86$ and $L_X(r < 2.25 \text{ Mpc})/L_X(r < 1.75 \text{ Mpc}) = 1.04$. Thus the Einstein and ASCA luminosity measurements are in reasonable agreement.

ASCA's angular resolution does not permit detailed mapping of the cluster surface brightness profile, so we use the mean observed surface brightness and plausible assumptions to infer the central gas density and total gas mass. Assuming a hydrostatic isothermal model with core radius $r_c = 0.25$ Mpc and $\beta = 0.65$, we find a central gas density $n_0 = 6.5 \times 10^{-3}$ cm^{-3}, and a total gas mass (within 2.25 Mpc) $M_{gas} = 3.2 \times 10^{14} M_\odot$. Independent density estimates obtained from the SIS and GIS, in the two different apertures described above, agree to within 5%. Although the estimate of n_0 is sensitive to the assumed core radius, the gas mass estimate is most sensitive to the assumed value of β, and to the assumption that the gas is smoothly distributed. A preliminary analysis of the ASCA profiles suggests $\beta = 0.65 \pm 0.15$. The corresponding uncertainty in the gas mass estimate is $\sim 25\%$. The cooling time for gas at the center of the cluster at the observed mean temperature is 1.6×10^{10} yr.

If the gas is isothermal, then, given the surface brightness parameters assumed above, we can estimate the

total cluster ("virial") mass (e.g., Cowie et al. 1987). We find $M_{\rm vir} = (1.5 \pm 0.4) \times 10^{15} M_{\odot}$ within a radius of 2.25 Mpc. Here again the principal uncertainty is the shape of the surface brightness profile; the uncertainty in the temperature contributes negligibly to the uncertainty in mass. The mass estimate is also sensitive to the assumption that the gas is isothermal; as discussed below, this assumption may not be valid. Nevertheless, our mass measurement is in remarkable agreement with the optically-determined virial mass $M_{\rm vir} = (1.5 \pm 0.4) \times 10^{15} M_{\odot}$ (Mellier et al. 1988). Our mass measurement is also consistent with a self-similar scaling argument, $M_{\rm vir} \sim T^{3/2}$, (David et al. 1993) applied to the Coma cluster.

The X-ray properties of A370 are similar in several respects to those of nearby clusters of comparable X-ray luminosity. The ratio of gas mass to cluster mass is $M_{\rm gas}/M_{\rm vir} = 0.21$. This value is consistent with that found for nearby clusters of comparable mass (Cowie et al. 1987; Hughes 1989). We observe that, as is the case for Coma, $M_{\rm gas}/M_{\rm vir} > \Omega_{\rm baryon}/\Omega_0$ if $\Omega_0 = 1$ (White et al. 1993). The emission-averaged temperature of the ICM in A370 is quite close the the value predicted by the luminosity-temperature relationship observed for nearby clusters. For example, the relationship quoted by David et al. (1993) predicts a temperature $kT = 7.8 \pm 0.8$ keV for a cluster with $L_{\rm X} = 1.3 \times 10^{45}$ erg s^{-1}. Finally this cluster has the "β problem," with a value of $(\sigma^2/kT) = 1.25$, similar to many low-z clusters.

The measured iron abundance for A370 is higher, at the 90% confidence level, than that predicted by the abundance-temperature correlation observed for nearby rich clusters (Hatsukade 1989; Arnaud et al. 1992). The most distant cluster in which iron line emission had been previously detected (at greater than 90% confidence) is A2507 ($z = 0.196$) (Arnaud et al. 1991). The present results thus extend by a large factor the lookback time at which iron has been observed in the intracluster medium.

The presence of iron in A370 is consistent with models in which type-II-supernova-driven winds from early-type galaxies are responsible for the bulk of the gas enrichment, since, in this picture, most of the enrichment occurs within a few times 10^8 yr of galaxy formation (Arnaud et al. 1992; David et al. 1991). Indeed, if the ICM is homogeneous, then we require no enrichment by type Ia supernovae between the epoch of observation and the present to account for the observed iron abundance in A370. More generally, in this case, the iron contributed to the ICM by continuing type Ia supernovae must be negligible compared to that injected before a lookback time of ~ 5 Gyr. On the other hand, as has been pointed out by Fabian et al. (1994), if the iron in the ICM is initially inhomogeneous, then subcluster merging may act to homogenize the ICM and thus lower the observed mean abundance. This potential evolutionary effect of merging thus makes it difficult to rule out the continuing enrichment of the ICM, particularly in the case of A370, in which gravitational images suggest that we may be observing two subclusters in proximity to one another (Kneib et al. 1993). In a forthcoming paper we investigate this point in more detail, and show that the ASCA data, together with the gravitational lens characteristics, are not consistent with an isothermal ICM in a unimodal potential.

While the iron abundance obtained directly from our X-ray spectrum measures the proportion of iron in the ICM, it is also useful to consider the relationship between the total mass of iron in the ICM and the (optical) characteristics of the cluster stellar population. Efforts to understand ICM enrichment mechanisms (e.g., by Arnaud et al. 1992; Renzini et al. 1993) have focussed on the ratio of iron mass to optical luminosity, $M_{\rm Fe}^{\rm ICM}/L_{\rm opt}$, which is found to be roughly the same for all low-z clusters. Although not well-constrained by the optical data, we find this ratio for A370 to be consistent with that observed in nearby clusters. Assuming that the iron abundance in the ICM is homogeneous, we estimate the total mass of iron to be $M_{\rm Fe}^{\rm ICM} = (2.1 \pm 0.6) \times 10^{11} M_{\odot}$. The optical luminosity distribution of A370 is known only in the central 0.9 Mpc radius (Mellier et al. 1988). If we extrapolate the measured galaxy density profile to a radius of 2.25 Mpc (which entails a factor of three correction to the optical luminosity), and make color corrections appropriate for early type galaxies, we find $M_{\rm Fe}^{\rm ICM}/L_{\rm B} = 0.01 (M_{\odot}/L_{\odot})$ for A370, which is within the range 0.01–0.02 reported by Renzini et al. (1993) for low-z clusters. Arnaud et al. (1992) find that $M_{\rm Fe}^{\rm ICM}$ is most tightly correlated with stellar mass (or luminosity) in early-type galaxies. Even allowing for the large proportion of star-forming galaxies in the core of A370 (approximately 50%; Mellier 1988), we find $M_{\rm Fe}^{\rm ICM}/L_{\rm V}^{\rm E,S0} = 0.015 (M_{\odot}/L_{\odot})$, well within the range found by Arnaud et al. (1992). Thus, the (rather lax) constraints imposed by the available optical measurements and the scatter in the observed correlations low-z clusters imply that the ratio $M_{\rm Fe}^{\rm ICM}/L_{\rm opt}$ does not evolve by more than a factor of two from $z = 0.4$ to the present epoch, even for a Butcher-Oemler cluster.

4. Summary

We have measured the mean temperature and iron abundance of the intracluster gas in the distant cluster of galaxies A370. The mean gas temperature and density, the gas mass and the total cluster mass are all similar to those of nearby clusters of comparable X-ray lumimnosity. We detect iron K line emission with high confidence, and establish for the first time the presence of iron in the intracluster medium at the epoch corresponding to $z \sim 0.4$. The relatively high iron abundance is consistent

with but does not require models in which all of the iron enrichment occurs before the epoch of observation.

We thank Michael Loewenstein for providing us with results of his research in advance of publication.

References

Abell G.O., Corwin H.G. Jr., Olowin R.P. 1989, ApJS 70, 1
Arnaud M., Lachièze-Rey M., Rothenflug R., Yamashita K., Hatsukade I. 1991, A&A 243, 56
Arnaud M., Rothenflug R., Boulade O., Vigroux L., Vangioni-Flam E. 1992, A&A 254, 49
Butcher H., Oemler A. Jr. 1984, ApJ 285, 426
Cowie L., Henriksen M., Mushotzky R. 1987, ApJ 317, 593
David L.P., Forman W., Jones C. 1991, ApJ 380, 39
David L.P., Slyz A., Jones C., Forman W., Vrtilek S.D., Arnaud K. 1993, ApJ 412, 479
Edge A.C., Stewart G.C., Fabian A.C., Arnaud K. 1990, MNRAS 245, 559
Fabian A.C., Crawford C., Edge A.C., Mushotzky R. 1994, MNRAS in press
Fabricant D.G., McClintock J.E., Bautz M.W. 1991, ApJ 381, 33
Gioia I.M., Henry J.P., Maccacaro T., Morris S.L., Stocke J.T., Wolter A. 1990, ApJL 356, L35
Hatsukade I. 1989, Ph.D. Thesis, Osaka University, ISAS Research Note 435
Henry J.P., Gioia I.M., Maccacaro T., Morris S.L., Stocke J.T., Wolter A. 1992, ApJ 386, 408
Hughes J.P. 1989, ApJ 337, 21
Jones C., Forman W. 1984, ApJ 276, 38
Kneib J.P., Mellier Y., Fort B., Mathez G. 1993, A&A 273, 367
Loewenstein M. 1994 ApJ in press
Lynds R., Petrosian V. 1986, Bul. AAS 18, 1014
Mellier Y., Soucail G., Fort B., Mathez G.,Cailloux M. 1988, A&A 199, 13
Paczynski B. 1987, Nature 325,572
Perrenod S.C., Henry J.P. 1981, ApJL 247, L1
Renzini A., Ciotti L., D'Ercole A., Pellegrini S. 1993, ApJ 419, 52
Ross J.E., Aller L.H. 1976, Science 191, 1223
Soucail G., Mellier Y., Fort B., Mathez G. 1987 IAU Circ. 4482,1
Stark A.A., Gammie C.P., Wilson R.W., Bally J., Linke R., Heiles C., Hurwitz M. 1992, ApJS 79, 77
Wang Q., Stocke J.T. 1993, ApJ 408, 71
White S.D.M., Navarro J.F., Evrard A.E., Frenk C.S. 1993, Nature 366 429